Ann. Geophysicae 13, 836–842 © EGS – Springer-Verlag 1995

Annales Geophysicae

Delay coordinates: a sensitive indicator of nonlinear dynamics in single charged particle motion in magnetic reversals

Sandra C. Chapman and Nicholas W. Watkins

Space Science Centre (MAPS), University of Sussex, Brighton BN1 9QH, UK

Received: 5 December 1994/ Revised: 21 March 1995/ Accepted: 23 March 1995

Abstract. The delay coordinate technique is examined as an indicator of the regime of particle dynamics for the system of single charged particle motion in magnetic reversals. Examples of numerically integrated trajectories in both static (zero electric field) and time dependent (corresponding nonzero induction electric field) simple models for magnetic reversals are considered. In the static case, the dynamics can in principle be directly classified by constructing Poincaré surfaces of section; here we demonstrate that whilst the Poincaré surface contains the relevant information to classify the dynamics, the corresponding delay coordinate plot can provide a far more sensitive indication of the onset of nonregular behaviour. In the case of nonperiodic time dependence considered here Poincaré plots cannot in general be constructed directly. Nevertheless, delay coordinate plots can still reveal details of the phase space portrait of the system, and here are shown to indicate whether segments of stochastic motion exist in a given trajectory. It is anticipated that the delay coordinate plot technique as realized here will be a valuable tool in characterizing the behaviour in large numbers of trajectories that are evolved in time-dependent systems, thereby giving us insight into the evolution of the distribution function as a whole, either in prescribed fields or in self-consistent numerical simulations.

1 Introduction

Techniques for the analysis of time series generated by nonlinear processes are becoming increasingly relevant to geophysical phenomena (see, for example, MacDowell, 1981 and references therein). Those techniques which are generally applicable and which do not rely heavily on a priori assumptions will be of particular value. One such technique is the delay coordinate plot (e. g. Shaw, 1984; Takens, 1981), which has already had some application to time series of global geomagnetic indices (see, for example, Sharma et al., 1993 and references therein).

Here we examine the application of this technique to a problem of considerable interest: that of single charged particle dynamics in magnetic reversals. There exists an extensive literature (e g. Speiser, 1965; Sonnerup, 1971; Chen, 1992; Buchner and Zelenyi, 1986; Buchner and Zelenyi, 1989; Wang, 1994) on the problem of single charged particle dynamics in simple static models of the magnetic field reversal in the earth's magnetotail. More recently, dynamics in smoothly varying (nonoscillatory), time dependent reversals (intended to model the presubstorm plasma sheet) have been investigated (Chapman and Watkins, 1993; Chapman, 1994). In the static parabolic model where the Hamiltonian H is a constant of the motion, the particle orbit has a given dynamical behaviour (it is either regular or stochastic) for all t, and different regimes of behaviour have been identified (Buchner and Zelenyi, 1986; Buchner and Zelenyi; 1989, Chen and Palmadesso, 1986). In a parabolic field, model with simple, nonoscillatory time dependence and a corresponding induction electric field (Chapman and Watkins, 1993; Chapman, 1994), a single trajectory may execute segments both of regular and stochastic behaviour at different times. Note that in this context, stochasticity implies that an orbit or segment of an orbit may access an extensive region in phase space, in contrast to a regular orbit, or segment of an orbit, which is constrained in phase space by the existence of the same number of exact and/or conserved adiabatic invariants as the number of degrees of freedom.

Analyses of the time series generated by numerically integrating the trajectories of charged particles in the static and time-dependent systems therefore present different problems, although in all cases, the key requirement is to select a reduced time series which characterizes the dynamics. A standard technique for static systems is to construct a Poincaré surface of section (see e. g. Lichtenberg and Lieberman, 1992; Chen and Palmadesso, 1986; Wang, 1994) which represents a 'cut' through the phase space torus of a given particle trajectory. The nature of this torus as revealed by the Poincaré plot thus describes in principle the nature of the dynamics, although, as we will demonstrate, this may be difficult to identify in practice. As the system is static, we can in principle integrate for arbitrarily large t to allow the trajectory to explore all accessible regions of the Poincaré surface of section. In a time-dependent system, this is no longer the case; in a smoothly time-varying system (i. e. in which the fields do not oscillate), the orbit is no longer constrained to constant H surfaces and can exhibit transient motion. An alternative means of analysing the trajectory time series is therefore required in

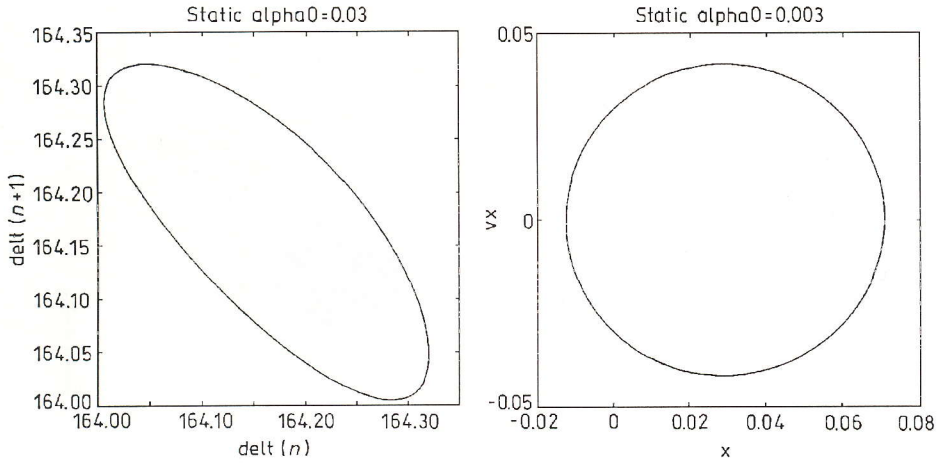

Fig. 1. Static model ($\alpha_0 = 0.03$): delay coordinate (left) and Poincaré (right) plots

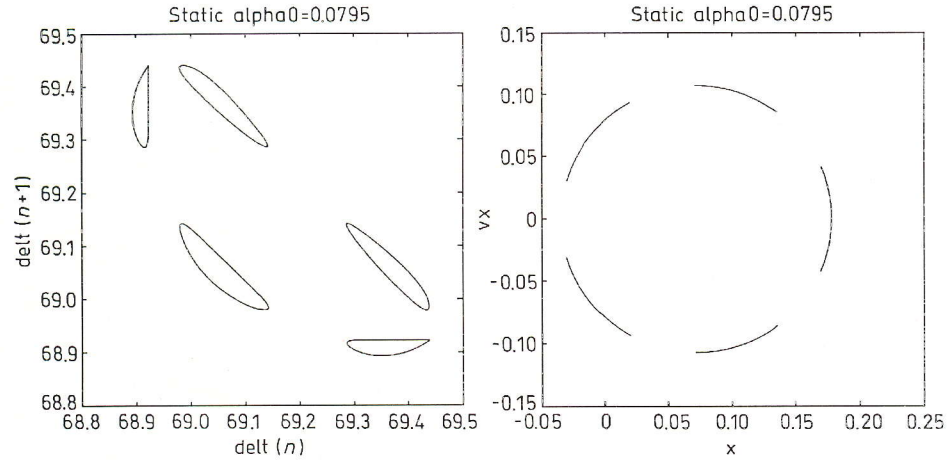

Fig. 2. Static model ($\alpha_0 = 0.0795$): delay coordinate (left) and Poincaré (right) plots

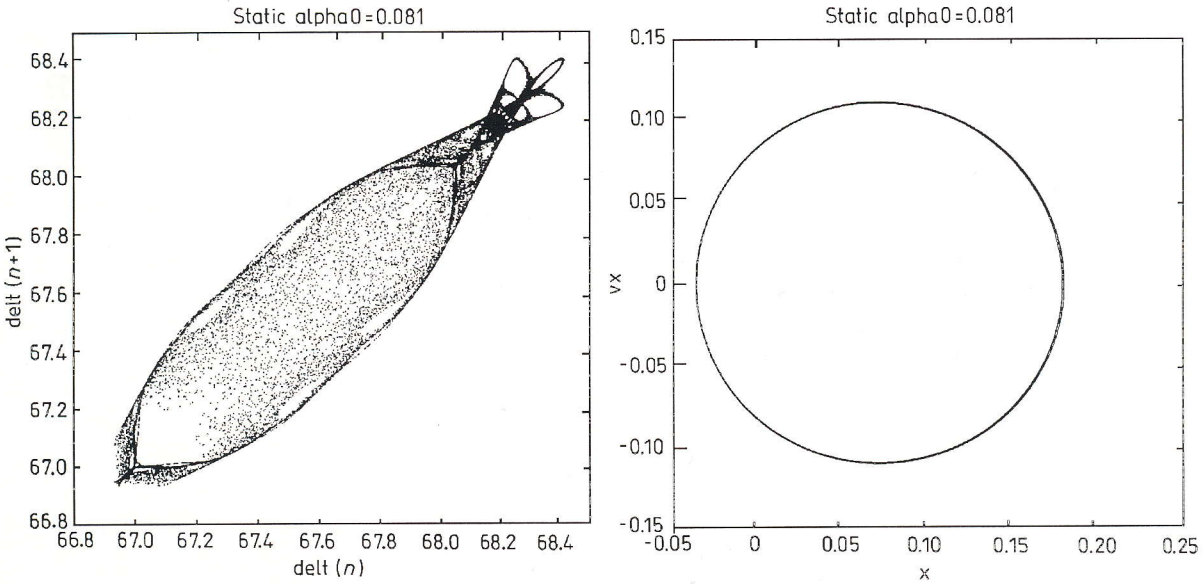

Fig. 3. Static model ($\alpha_0 = 0.081$): delay coordinate (left) and Poincaré (right) plots

order to investigate the dynamical properties of trajectories in time-dependent systems of this type.

2 Reduced time series from phase space trajectories

In a static system, the complete particle trajectory obtained over some arbitrarily long time interval in a given field model maps out a torus, in general, in six-dimensional phase space, given by canonical coordinates $\mathbf{p}(t)$ and $\mathbf{q}(t)$, where t is a parametric coordinate only (i.e. a regular trajectory will correspond to a torus with a simple surface). A time series which is a numerically integrated trajectory of m points $\mathbf{p}_j$ and $\mathbf{q}_j$, $j = 1, m$ will in some sense sample this torus (i.e. the m points will lie close to the torus surface). The dynamics of the trajectory can be characterized by examining the nature of the torus surface, which can be revealed from a surface of section through the torus surface and does not require the entire torus to be known. This Poincaré surface of section (Poincaré plot) is then defined formally by setting one of the phase space coordinates (one of the components of $\mathbf{p}$ or $\mathbf{q}$) to a constant (in the examples to be given here, zero). Numerically, n points on the trajectory, which lie on the surface of section, are obtained from a subset of the original m points by interpolation, providing a reduced time series. Once the surface of section is defined, the times t_n at which the particle trajectory crosses it provides an alternative reduced time series. This time series is not independent of that required for the Poincaré plot itself, since in the static system, t is a parametric (not an independent) coordinate on the trajectory. The delay coordinate plot for this irregularly spaced time series is obtained by plotting successive intervals between crossings of the surface of section, i.e. $delt(n+1) = t_{n+2} - t_{n+1}$ versus $delt(n) = t_{n+1} - t_n$. Such a plot essentially reveals structure in the frequency information in the particle trajectory as it executes repeated cycles around the phase space torus.

In the explicitly time dependent system, the coordinate t is no longer dependent on the other six phase space coordinates. The $\mathbf{p}$, $\mathbf{q}$ of the trajectory do not map out a static torus in phase space. However, we can still define a surface of section by setting one of the components of $\mathbf{p}$ or $\mathbf{q}$ to zero, and obtain the reduced time series t_n of the times at which the particle trajectory crosses the surface of section. The t_n can again be used to construct a delay coordinate plot which will reveal structure in the frequency information of the trajectory.

We will now examine the reduced time series from numerically integrated trajectories in simple field models in which the magnetic field reverses. The integration was performed using a variable order, variable stepsize technique (as in Chapman and Watkins, 1993). Coordinate plots have not previously been presented. Normalizing the magnetic field to the linking field B_z, temporal scales to the inverse of the gyrofrequency in this field $\Omega_z = \frac{eB_z}{m}$ and spatial scales to the particle gyroradius $\rho_z = \frac{v}{\Omega_z}$, the static parabolic field model is:

$$\mathbf{B} = (\alpha_0 z, 0, 1), \tag{1}$$

with $\mathbf{E} = 0$ in the de-Hoffman-Teller frame and where

$$\alpha_0 = \frac{B_{x0}}{B_z}\frac{\rho_z}{h_0}. \tag{2}$$

The Hamiltonian is

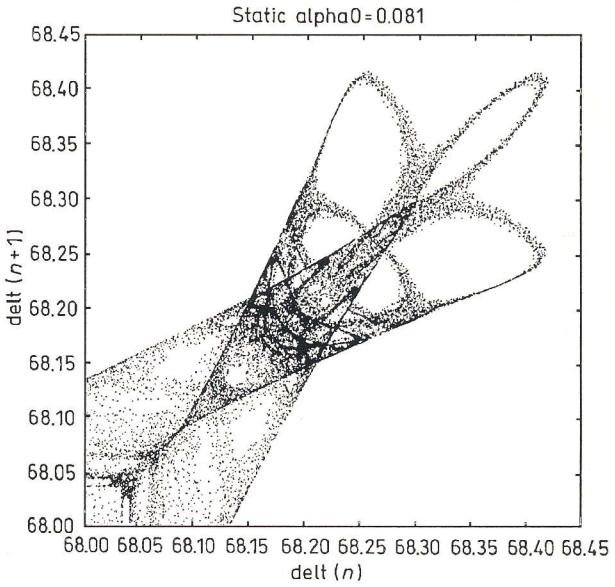

Fig. 4. Static model ($\alpha_0 = 0.081$): structure in the delay coordinate plot: a zoom of the left-hand plot of Fig. 3

$$H_0 = \frac{\dot{x}^2}{2} + \frac{\dot{z}^2}{2} + \Psi_0(\alpha_0, x, z), \tag{3}$$

where the pseudopotential has implicit time dependence only i.e.

$$\Psi_0 = \frac{1}{2}(\alpha_0\frac{z^2}{2} - x)^2 = \frac{1}{2}A^2, \tag{4}$$

so that the canonical coordinates of the system are simply $p_1 = \dot{x}$, $p_2 = \dot{z}$, $q_1 = x$, $q_2 = z$. The parameter α_0 measures the degree of nonintegrability in the sense that $\alpha_0 \to 0$ is an integrable limit in which the normalized pseudopotential becomes $\Psi_0 = \frac{1}{2}x^2$, corresponding to simple harmonic motion (gyration) about the the linking field B_z, with a zero reversing field $B_x = 0$ (or an infinite sheet thickness compared to the gyroradius $\frac{h}{\rho_z} \to \infty$). The other limit, of vanishing linking field $B_z = 0$ so that $\alpha_0 \to \infty$, cannot legitimately be taken under this normalization; under a different normalization (i.e. to the reversing field B_{x0} instead of the linking field B_z), the integrable limit of serpentine motion in a neutral sheet may be recovered.

For small values of α_0, the system might therefore be expected to be close to integrable, and if chaotic, small changes in α_0 will yield substantial changes in the dynamics. The system therefore provides a convenient illustration of the application of both Poincaré and delay coordinate plots, which have been constructed here for the surface of section $q_2 = z = 0$, which is the centre plane of the reversal. This surface is convenient since in this parabolic model, all particles remain trapped and will continually cross the centre plane.

Examples of delay coordinate plots for different values of α_0 are shown in Figs. 1–7. In each case, the particle was started at the origin, at 45° pitch angle and at normalized speed of 1. The corresponding Poincaré plots, constructed from the $\dot{x}$, x coordinates of the trajectories as they cross the $z = 0$ plane, are also shown. The method can be seen to reveal markedly different characteristic structures in frequency space for small changes in α_0. A regular trajectory is shown in

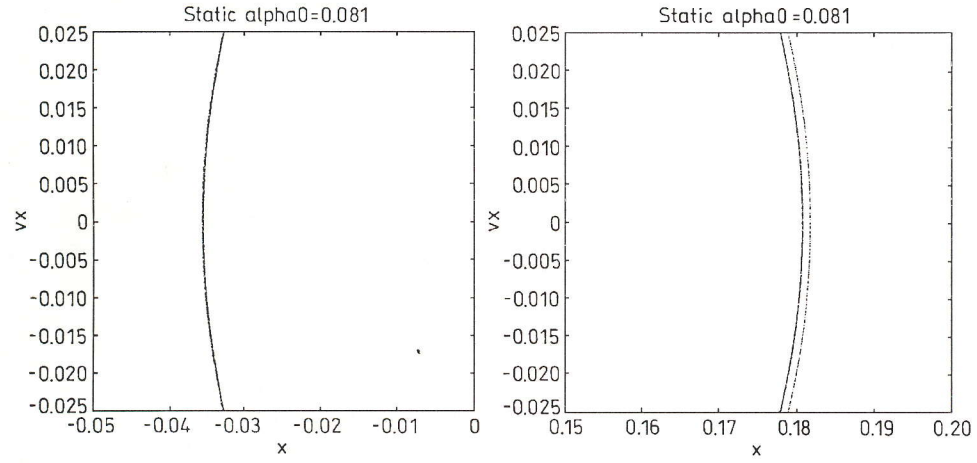

Fig. 5. Static model (α_0 = 0.081): a zoom of the Poincaré plot (right-hand plot) in Fig. 3, which shows two distinct resonant surfaces (right) which overlap (left)

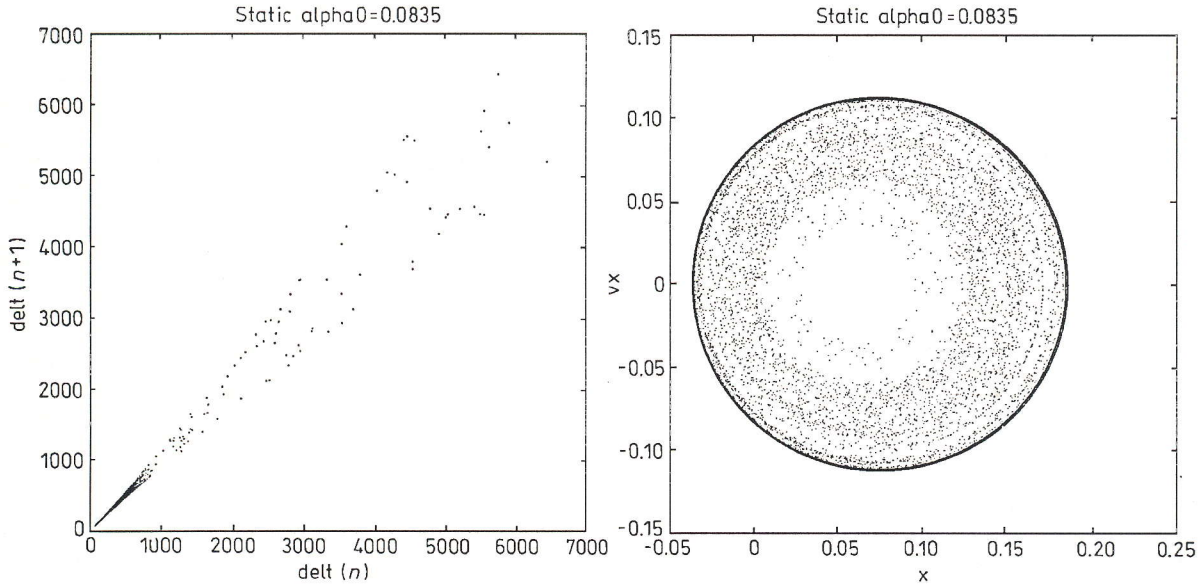

Fig. 6. Static model (α_0 = 0.0835): delay coordinate (left) and Poincaré (right) plots

Fig. 1, constructed for $\alpha_0 = 0.03$. Here both the Poincaré surface of section and the delay coordinate plot have the same geometric property; that is the particle remains on a single closed surface. Fig. 2 shows the dynamics for a slightly larger value of $\alpha_0 = 0.0795$. Here the single trajectory threads each of the five accessible regions of the $\dot{x}, x$ Poincaré surface in turn; that is, they represent a single surface rather than five disconnected islands. Again, the delay coordinate plot reproduces the geometry of the Poincaré plot.

A signature of the onset of nonregular dynamics in the Poincaré plot is the appearance of resonant tori (which overlap in phase space). Regular trajectories will be confined to nested tori in phase space that do not overlap, each torus being specified by exact and/or well-conserved adiabatic invariants. When two nearby tori appear to overlap, a single trajectory has access to surfaces in phase space associated with two different values of these adiabatic invariants, so that we observe 'jumps' in at least one adiabatic invariant if we follow the trajectory in time. This occurs for a slightly larger value of $\alpha_0 = 0.081$, shown in Figs. 3–5. The distinct but overlapping tori are difficult to resolve on the Poincaré surface of section in its entirety, shown in Fig. 3, but can be seen by enlarging sections of it (Fig. 5). The delay coordinate plot, on the other hand, immediately reveals the fundamentally different geometry of this particle orbit by its complex structure. The detail in the structure is shown in an enlargement in a section of the delay coordinate plot, in Fig. 4. Since the coordinates of each point on the delay coordinate plot are a pair of two sucessive half-bounce periods (sucessive intervals between crossings of the $z = 0$ plane), the plot gives a reduced set of the frequency information in the trajectory. Complex structure in the delay coordinate plot is thus equivalent to complex structure in the frequency spectrum of the trajectory time series, which is indicative of the particle's irregular motion as it moves on the surface of the resonant tori in phase space. This complex structure is generated by the topologically complex surface produced when the two simple surfaces of the two tori overlap; although the overlapping surface itself (shown in detail on the left hand plot of Fig. 5) appears to have simple properties. The range of times between crossings is small, varying by less than 1%, and the change in pitch angle (i. e. the jump in μ) is also extremely small, so that a plot of the particle xyz

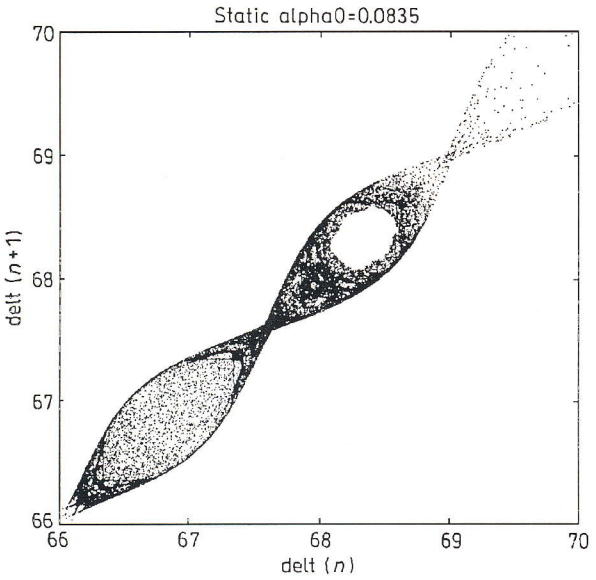

Fig. 7. Static model ($\alpha_0 = 0.0835$): structure in the delay coordinate plot (a zoom of the bottom left region of the delay coordinate plot in Fig. 6)

trajectory would suggest dynamics that were identical to that of the regular trajectory. The delay coordinate plot is hence an extremely sensitive indicator of the topological properties of the system.

A further small increase in α_0, to $\alpha_0 = 0.0835$, produces a particle orbit which begins to show some stochasticity, as shown in Figs. 6 and 7. A large region of the Poincaré surface of section is now accessible to the trajectory. The particle is strongly pitch-angle scattered and has times between crossings ranging over three orders of magnitude, as can be seen in the delay coordinate plot. An enlargement of the bottom left-hand corner of the delay coordinate plot, shown in Fig. 7, also reveals that the orbit is not completely stochastic and that much of it is confined to a complex surface similar to the previous trajectory; this surface is located at the outside edge of the accessible region shown on the Poincaré plot.

3 Simple time-dependent model

We will consider a magnetic field which is of the form:

$$\mathbf{B} = \left(f_x(T) B_{x0} \frac{Z}{h}, 0, f_z(T) B_z \right); \tag{5}$$

that is, with the same spatial dependence as the static model, but with additional, smoothly varying (i.e. non oscillatory) time dependence given by dimensionless functions f_x and f_z. Using the same normalization as in the static model, this gives

$$\mathbf{B} = \left(f_x\left(\frac{t}{\Omega_z}\right) \alpha_0 z, 0, f_z\left(\frac{t}{\Omega_z}\right) \right), \tag{6}$$

with

$$\mathbf{A} = f_z\left(\frac{t}{\Omega_z}\right) x - f_x\left(\frac{t}{\Omega_z}\right) \alpha_0 \frac{z^2}{2} + A_t\left(\frac{t}{\Omega_z}\right) \hat{\mathbf{y}}, \tag{7}$$

with corresponding induction electric field

$$\mathbf{E} = -\frac{\partial \mathbf{A}}{\partial T}. \tag{8}$$

Here, α_0 is as defined for the static model and the frame-dependent convectional $E_c(T) = -\dot{A}_t(T)$, which in general cannot be removed by a de-Hoffman-Teller frame transformation. The time-dependent Hamiltonian equation of motion is

$$\dot{H} = \frac{d}{dt}\left(\frac{1}{2}(\dot{x}^2 + \dot{z}^2) + \Psi \right) = \mathbf{v}.\mathbf{E} = \frac{\partial \Psi}{\partial t}, \tag{9}$$

with a pseudopotential that now has explicit time dependence

$$\Psi = \frac{1}{2} A_y^2 = \frac{1}{2} f_z^2 \left(x - \frac{f_x}{f_z} \alpha_0 \frac{z^2}{2} + \frac{A_t}{f_z} \right)^2. \tag{10}$$

The system has the same canonical coordinates as the static model, the time dependence resulting in a pseudopotential which, as well as having the same spatial dependence as in the static model, is a function of time-dependent parameters $\lambda_1(t) = \alpha_0 f_x / f_z$ and $\lambda_2(t) = f_z$ and of the frame-dependent $A_t(t)$. The Hamiltonian equation of motion can be shown to yield regular behaviour in the limit $f_x \to 0$, f_z finite, i.e. $\lambda_1 \to 0$ or in the limit $f_z \to 0$, f_x finite., i,e. $\lambda_1 \to \infty$; hence, a single trajectory can at different times be within one or the other of these limits. These limits will correspond to the regular oscillatory solutions of gyromotion about the z component of the field, and to serpentine motion in the neutral sheet (i.e. the x component of the field) if the rate of change of Ψ is sufficiently small. The rate of change of Ψ has been quantified with two parametric coordinates,

$$d\lambda_1(t) = \frac{|\dot{\lambda}_1|}{\lambda_2}, \tag{11}$$

and

$$d\lambda_2(t) = \frac{|\dot{\lambda}_2|}{\lambda_2^2}, \tag{12}$$

(Chapman and Watkins, 1993; Chapman, 1994), which appear since there are two timescales on which the pseudopotential changes. These timescales are just the characteristic particle Larmor period given by $\lambda_2 = \omega_x = f_z$, and the timescale for a transition in dynamics given by the time taken for $\lambda_1 \ll 1$ to $\lambda_1 \to 1$ as measured by this Larmor period.

If both $d\lambda_1 \ll 1$ and $d\lambda_2 \ll 1$ throughout the transition from the $\lambda_1 \to 0$ to the $\lambda_1 \to \infty$ limits ('slow passage'), the limits can yield regular motion, and for finite λ_1, segments of stochastic behaviour can occur. If either $d\lambda_1 \gg 1$ or $d\lambda_2 \gg 1$ through the transition ('fast passage'), the motion may no longer be stochastic.

This property should be identifiable by delay coordinate plots generated numerically for specific models. A model has been selected which has the property that $\lambda_1 = \lambda_1(t)$, $d\lambda_1 = d\lambda_1(t)$, and $d\lambda_2$ is constant; trajectories in this model then exhibit transitions with respect to both λ_1 and $d\lambda_1$ and are ordered with respect to $d\lambda_2$. Using the above normalization, the magnetic field is

$$\mathbf{B} = \left(\alpha_0 z, 0, \frac{1}{\left(\frac{t_0}{\Omega_z} + \frac{t}{\Omega_z \tau} \right)} \right), \tag{13}$$

which represents a 'thinning' field; that is, the linking field decreases with t. The corresponding electric field has $E_c(T) = 0$, this corresponds to a frame of reference in which the field

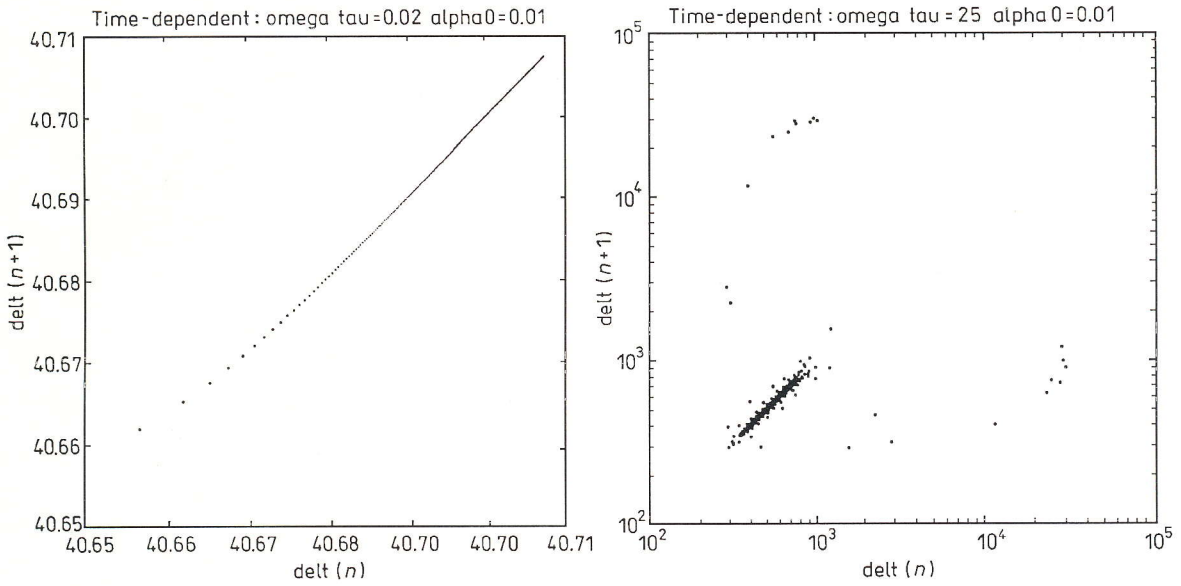

Fig. 8. Time-dependent model: the left-hand plot shows a fast transition, the right-hand plot, a slow transition

line passing through $X = 0$, $Z = 0$ is at rest. The parametric coordinates for this system are

$$\lambda_1 = \alpha_0 \left(\frac{t_0}{\Omega_z} + \frac{t}{\Omega_z \tau} \right), \tag{14}$$

$$\lambda_2 = \frac{1}{\left(\frac{t_0}{\Omega_z} + \frac{t}{\Omega_z \tau} \right)}, \tag{15}$$

$$d\lambda_1 = \frac{1}{\Omega_z \tau} \lambda_1, \tag{16}$$

$$d\lambda_2 = \frac{1}{\Omega_z \tau}. \tag{17}$$

It should be noted that $\lambda_1 \not\to 0$ as $t \to 0$; so that the model does not contain the $\lambda_1 \to 0$ regular limit of gyromotion in a spatially uniform z field, but does potentially contain the $\lambda_1 \to \infty$ regular limit of serpentine motion in a neutral sheet at $t \to \infty$. We therefore chose initial values for the trajectories with $t = 0$ and $t_0/\Omega_z \ll 1$; that is $\lambda_1 \ll 1$, so that the behaviour may be nearly regular (or weakly stochastic) at early t and can then pass through a segment of nonregular motion (if the transition is slow), i. e. when $\lambda_1 \sim 1$ at later t.

For the delay coordinate plots shown in Fig. 8, the field model has $\alpha_0 = 0.01$ (a weak reversal) and for the left hand plot $\Omega_z \tau = 0.02$, $d\lambda_2 = 50$ (a fast changing reversal) and for the right hand plot $\Omega_z \tau = 25$ $\lambda_2 = 0.04$ (a slowly changing reversal). In both cases, $t_0/(\Omega_z) = 0.01$, and the particle has initial position $\mathbf{r} = (5 \times 10^{-2}, 0, 1)$, such that initially the particle lies on the rest field line defined by the choice of $E_c(T) = 0$. The initial $\mathbf{v} = (0, 0.5, -0.01)$ at $t = 0$, with the velocity components chosen to ensure that the particle crosses the centre plane $z = 0$ on a shorter timescale than the transition timescales of the system. The delay coordinate plots clearly distinguish between the fast and slow transition; the left-hand plot reveals a system with a single frequency component that slowly changes with time ($d\lambda_2 \gg 1$ for all t), whereas the right-hand plot shows a period during which there is a wide range of frequencies, corresponding to the period when $\lambda_1 \sim 1$ and $d\lambda_1 < 1$ ($d\lambda_2 \ll 1$ for all t).

4 Summary

We have shown examples of how delay coordinate plots can be used to establish the nature of the dynamics of a single particle in a magnetic reversal. In the case of a static reversal, we have produced delay coordinate plots for small values of α_0 (close to a known integrable limit). These plots reveal dramatic changes in the dynamics for small incremental changes in α_0 and detailed structure in the frequency information of the trajectory, consistent with being in the parameter range for the onset of the destruction of KAM surfaces. In the case of a time-dependent reversal, the plots clearly show the distinction between systems which have the same α_0 but distinct (i. e. fast or slow) rates of change, as determined by adiabaticity parameters for the system.

It is anticipated that the delay coordinate plot technique will be useful in exploring dynamics in time-dependent models of magnetic reversals. In order to determine the importance of this dynamics for the presubstorm evolution of the thin current sheet in the earth's geotail, for example, it will be necessary to evolve large numbers of particle trajectories in the system to investigate the evolution of the distribution function of the plasma. This may be performed either in prescribed models for the electromagnetic field, or selfconsistently. In either case, a technique is required which reduces the trajectory time series whilst retaining sufficient information to characterize their dynamical properties.

A second application which is currently under study is the analysis of particle dynamics in self-consistent numerical simulations of nonlinear wave particle interactions using particle in cell codes. Time intervals between subsequent crossings of a given plane in phase space, defined as the plane in which one of the canonical position or momentum coordinates is constant and chosen to be a plane about which trapped particles precess can again be used to construct a reduced time

series for a trajectory. Trapping of particles in real space (i. e. Langmuir resonance) can be examined by choosing $q_k = 0$ in the wave frame, where this position coordinate is along the wave vector. Trapping in phase space (e. g. electron-whistler resonance) can be examined by choosing p_k as the component of velocity given by the resonance condition $\omega - \mathbf{v}.\mathbf{k} = n\Omega$. A delay coordinate plot constructed in this way will extract the trapping frequency directly from the trajectories of the computational particles.

Acknowledgement. The Editor-in-Chief thanks Th. Speiser ans another referee for their assistance in evaluating this paper.

References

Buchner, J., and L. M. Zelenyi, Deterministic chaos in the dynamics of charged particles near a magnetic field reversal, *Phys. Lett. A*, **118**, 395, 1986.

Buchner, J., and L.M. Zelenyi, Regular and chaotic charged particle motion in magnetotaillike field reversals, 1: Basic theory of trapped motion, *J. Geophys. Res.*, **94**, 11821, 1989.

Chapman, S. C., and N. W. Watkins, Parameterization of chaotic particle dynamics in a simple time-dependent field reversal, *J. Geophys. Res.*, **98**, 165, 1993.

Chapman, S. C., Properties of single particle dynamics in a parabolic magnetic reversal with general time dependence, *J. Geophys. Res.*, **99**, 5977, 1994.

Chen, J., and P. Palmadesso, Chaos and nonlinear dynamics of single particle orbits in a magnetotail like magnetic field, *J. Geophys. Res.*, **91**, 1499, 1986.

Chen, J., Nonlinear dynamics of charged particles in the magnetotail, *J. Geophys. Res.*, **97**, 15011, 1992.

Lichtenberg, A. J. and M. A. Lieberman, *Regular and Chaotic Dynamics*, second edition, Springer-Verlag, Berlin Heidelberg New York, 1992.

MacDowell, G. J., Spectral analysis of time series generated by nonlinear processes, *Rev. Geophys.*, **27**, 449, 1989.

A. S. Sharma, D. V. Vassiliadis and K. Papadopoulos, Reconstruction of low dimensional magnetospheric dynamics by singular spectrum analysis, *Geophys. Res. Lett.*, **20**, 335, 1993.

Shaw R., The dripping faucet as a model chaotic system, *Science Frontier Express Series*, Aerial Press, Santa Cruz, 1984.

T.W. Speiser, Particle trajectories in model current sheets, *J. Geophys. Res.*, **70**, 4219, 1965.

B. U. O. Sonnerup, Adiabatic orbits in a magnetic null sheet, *J. Geophys. Res.*, **76**, 8211, 1971.

Takens, F., "Detecting Strange Attractors in Tubulence", in *Lecture Notes in Mathematics 898*, D.A. Rand and L.S. Young, eds, Springer, Berlin Heidelberg New York, 1981.

Wang, Z.-D., Single particle dynamics of the parabolic field model, *J. Geophys. Res.*, **99**, 5949, 1994.

This article was processed by the author using the LaTeX style file *pljour2* from Springer-Verlag.